

# AN EFFICIENT QUADRATURE RULE ON THE CUBED SPHERE

BRICE PORTELENELLE AND JEAN-PIERRE CROISILLE †‡

**ABSTRACT.** A new quadrature rule for functions defined on the sphere is introduced. The nodes are defined as the points of the Cubed Sphere. The associated weights are defined in analogy to the trapezoidal rule on each panel of the Cubed Sphere. The formula enjoys a symmetry property ensuring that a proportion of 7/8 of all Spherical Harmonics is integrated exactly. Based on the remaining Spherical Harmonics, it is possible to define modified weights giving an enhanced quadrature rule. Numerical results show that the new quadrature is competitive with classical rules of the literature. This second quadrature rule is believed to be of interest for applied mathematicians, physicists and engineers dealing with data located at the points of the Cubed Sphere.

*Keywords:* Quadrature rule on the sphere ; Cubed Sphere ; Spherical Harmonic.

*Mathematics Subject Classification:* 33C55, 41A55, 65D30, 65D32

## 1. INTRODUCTION

In this paper we consider quadrature rules for functions defined on the sphere. Let  $\mathbb{S}^2$  be the unit sphere, and let  $\mathbf{x} \in \mathbb{S}^2 \mapsto f(\mathbf{x})$  be a regular function. A quadrature rule  $Q(f)$  is defined by

$$(1) \quad I(f) = \int_{\mathbb{S}^2} f(\mathbf{x}) d\sigma(\mathbf{x}) \simeq \sum_{p=1}^P w_p f(\mathbf{x}_p) = Q(f),$$

where  $\mathbf{x}_p \in \mathbb{S}^2$  are the nodes and  $w_p$  are the weights. The quest for rules of the form (1) has been a longstanding topic of interest. The classical setup of the problem consists in finding a minimal number  $\mathcal{P}$  of nodes  $x_p$  with the associated weights  $w_p$  for (1) to be as exact as possible. More precisely, the problem is to determine the location on the sphere of a minimal number of nodes for the largest number of Spherical Harmonics to be exactly integrated. A classical reference is [13]. Recent works on this topic include [16, 11, 1, 8]. For a general presentation of the problem we refer to the review chapters [9, Chap. 40] and [2, Chap. 5].

Here we consider the problem with a slightly different point of view. Over the past 20 years, the Cubed Sphere (see Fig.1) has become a popular spherical grid among researchers dealing with mathematical or physical models. In particular, in numerical climatology, the Cubed Sphere serves for various numerical schemes for time-dependent climate models on the sphere [12, 3, 17]. In this context, accurately evaluating averaged quantities over the sphere such as mass, momentum, energy or total vorticity is particularly important. This is in particular the case for the finite difference scheme introduced in [5, 6]. This scheme uses discrete unknowns located at the points of the Cubed Sphere. To use with this scheme, it is important to have a quadrature rule with nodes  $\mathbf{x}_p$  selected as the points of the Cubed Sphere.

To fully determine such a rule, it remains to identify a set of suitable weights  $w_p$ . A basic observation is that a particularly simple set of weights  $w_p$ , described hereafter, provides a rule (1), which is exact for a proportion of 7/8 of *all* Spherical Harmonics. Furthermore, for the remaining

---

*Date:* May 10, 2017.

This work was performed during the master thesis of the first author at the Univ. Lorraine, Math. Dept., Institut Elie Cartan de Lorraine in Metz, France, during the second semester of the academic year 2015-2016.

1/8 Spherical Harmonics not integrated exactly, fourth order accuracy convergence of the rule was numerically obtained. This observation was the starting point of the present study. Building upon this first rule (called  $Q_a$ ), we suggest a second rule  $Q_b$ , which keeps the 7/8 property and appears to be remarkably accurate.

The outline of the paper is as follows. Section 2 gives the notation for the Spherical Harmonics and the Cubed Sphere. In Section 3, our first quadrature rule, called  $Q_a$ , is introduced and the aforementioned 7/8 property is proved. This property is actually due to a set of combined symmetries shared by the Cubed Sphere and the Spherical Harmonics. In Section 4, we show how this property can serve to significantly enhance the selection of the weights associated with the nodes of the Cubed Sphere. This permits to define a second quadrature rule, called  $Q_b$ , which again uses the Cubed Sphere points as quadrature nodes. The weights  $w_p$  are selected according to a specific least square problem. Numerical results show that the rule performs very well compared to other spherical quadrature rules of the literature.

## 2. NOTATION

Consider the reference Cartesian frame  $\mathcal{R} = (\mathbf{O}, \mathbf{i}, \mathbf{j}, \mathbf{k})$  in  $\mathbb{R}^3$ . The unit sphere is  $\mathbb{S}^2 = \{\mathbf{x}(x, y, z) \in \mathbb{R}^3 | x^2 + y^2 + z^2 = 1\}$ . The Longitude-Latitude coordinate system is called  $(\lambda, \theta)$ , with  $-\pi \leq \lambda < \pi$  and  $-\pi/2 \leq \theta \leq \pi/2$ . For  $n \geq 0$  and  $m$  with  $-n \leq m \leq n$ , the Spherical Harmonic  $Y_n^m : \mathbf{x} \in \mathbb{S}^2 \mapsto Y_n^m(\mathbf{x}) \in \mathbb{C}$  is defined by [10, 2]:

$$(2) \quad Y_n^m(\mathbf{x}) = (-1)^m N_n^{|m|} P_n^{|m|}(\sin \theta) e^{im\lambda}.$$

For  $0 \leq m \leq n$ , the function  $x \in [-1, 1] \mapsto P_n^m(x)$  is the *associated Legendre polynomial*. It is defined in terms of the Legendre polynomial  $P_n(x) = \frac{d^n}{dx^n} \left( (x^2 - 1)^n \right) / (2^n n!)$  by the relation:

$$(3) \quad P_n^m(x) = (1 - x^2)^{m/2} \frac{d^m}{dx^m} P_n(x), \quad 0 \leq m \leq n, x \in [-1, 1].$$

The Spherical Harmonics form an orthonormal basis of the space  $L^2(\mathbb{S}^2)$  and therefore the integrals  $I(Y_n^m)$  are:

$$(4) \quad I(Y_n^m) = 0 \text{ if } (n, m) \neq (0, 0), \quad I(Y_0^0) = \sqrt{4\pi}.^1$$

The normalisation constant  $N_n^m$  in (2) is

$$(5) \quad N_n^m = \left( \frac{2n+1}{4\pi} \frac{(n-m)!}{(n+m)!} \right)^{\frac{1}{2}}.$$

A quadrature rule is usually designed using the functions  $Y_n^m$ . The accuracy is measured by the order  $n$  such that the functions  $Y_n^m(\mathbf{x})$ ,  $|m| \leq n$ , are integrated exactly.

Our next ingredient is a particular grid of  $\mathbb{S}^2$  called the Cubed Sphere (see Fig. 1). The Cubed Sphere with parameter  $N$  consists of  $6N^2 + 2$  points located on six panels, called  $\mathcal{P}^k$ , ( $I \leq k \leq VI$ ). These six panels match the six faces of the cube  $[-1, 1]^3$  embedding the sphere. This is the reason of the terminology *Cubed Sphere*. The topology of the six panels of the unfolded Cubed Sphere is shown on Fig. 2.

Each panel  $\mathcal{P}^k$  has a square shape represented on Fig. 3. It is supplied with a coordinate system  $(\xi, \eta)$ , whose coordinate lines are great circle sections. The coordinate lines  $\xi = 0$ , (resp.  $\eta = 0$ ) represent the vertical (resp. horizontal) equatorial line at the center of  $\mathcal{P}^k$ . The function  $\varphi_k$  is the bijective application defined by

$$(6) \quad \varphi_k : (\xi, \eta) \in \left[ -\frac{\pi}{4}, \frac{\pi}{4} \right]^2 \mapsto \mathbf{x}(\xi, \eta) \in \mathcal{P}^k.$$

<sup>1</sup>The function  $Y_0^0$  is the constant  $\frac{1}{\sqrt{4\pi}}$

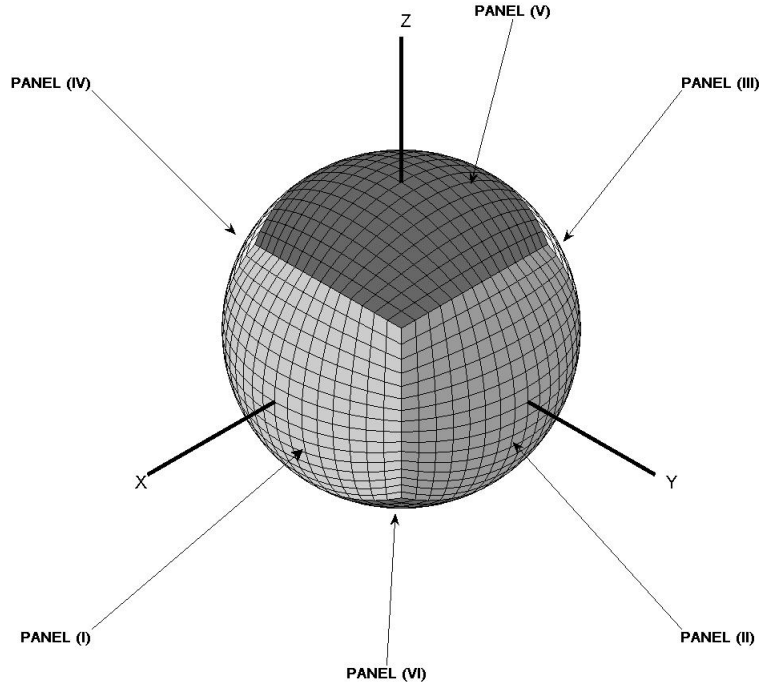


FIGURE 1. The Cubed Sphere with grid parameter  $N = 16$ . The total number of gridpoints is  $6 \times N^2 + 2 = 1538$  in this case. The panels (I), (II), (III) and (IV) are located around the equatorial plane  $z = 0$ . The index of the north panel is (V) and the one of the south panel is (VI).

Consider for example the case of the function  $\mathbf{x}(x, y, z) = \varphi_{(I)}(\xi, \eta)$  which defines panel (I). With the variables  $X = \tan(\xi)$  and  $Y = \tan(\eta)$ , the components  $x$ ,  $y$  and  $z$  of  $\varphi_1$  are defined by

$$(7) \quad x = \frac{1}{\sqrt{1 + X^2 + Y^2}}, \quad y = \frac{X}{\sqrt{1 + X^2 + Y^2}}, \quad z = \frac{Y}{\sqrt{1 + X^2 + Y^2}}.$$

Similar relations hold for the five other panels [14]. On each panel  $\mathcal{P}^k$ , the metric tensor  $G$  [15] is expressed in terms of  $X$  and  $Y$  by

$$(8) \quad G(\xi, \eta) = \frac{(1 + X^2)(1 + Y^2)}{(1 + X^2 + Y^2)^2} \begin{bmatrix} 1 + X^2 & -XY \\ -XY & 1 + Y^2 \end{bmatrix}.$$

The determinant is

$$(9) \quad \det G(\xi, \eta) = \frac{(1 + X^2)^2(1 + Y^2)^2}{(1 + X^2 + Y^2)^3}.$$

The restriction of the Cubed Sphere to  $\mathcal{P}^k$  consists of the  $(N + 1)^2$  points  $\mathbf{s}_{i,j}^k$  defined for  $k = (I), \dots, (VI)$  and  $-N/2 \leq i, j \leq N/2$ ,<sup>2</sup>

<sup>2</sup>We assume for simplicity that  $N$  is an even integer.

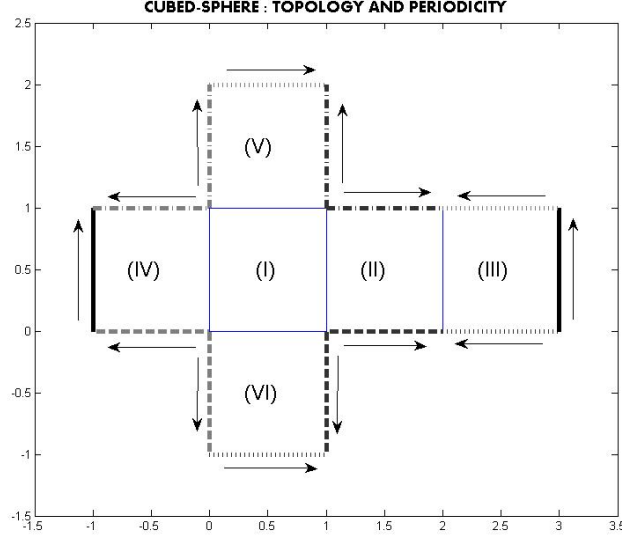


FIGURE 2. The topology and spherical periodicity of the six panels is displayed on the unfolded Cubed Sphere. The Latin numbers (I), (II), (III), (IV), (V) and (VI) designate the number of the panels from  $k = (I)$  to  $k = (VI)$ . Each of the 12 edges of the Cubed Sphere is represented by a couple of segments on the picture, indicated by one of the four symbols (—, - · -, ... or —) and one of the two colors (black or grey). The arrows indicate how the edges are defined from each pair of segments with the same symbols.

by

$$(10) \quad \begin{cases} \mathbf{s}_{i,j}^k = \varphi^k(\xi_i, \eta_j), \\ \Delta\xi = \Delta\eta = \pi/2N, \\ \xi_i = i\Delta\xi, \quad \eta_j = j\Delta\eta. \end{cases}$$

The points of the Cubed Sphere consist of the points  $(\mathbf{s}_{i,j}^k)$  with  $-\frac{N}{2} \leq i, j \leq \frac{N}{2}$  and  $(I) \leq k \leq (VI)$ . As shown on Fig. 3, the points on each panel are classified as *internal* points, *edge* points and *corner* points. Therefore by summing up over panels (I) to (VI) the  $(N+1)^2$  points, one counts two times the  $12(N-1)$  edge points and three times the 8 corner points. This leads to a number of  $6N^2+2 = 6 \times (N+1)^2 - 12 \times (N-1) - 2 \times 8$  points. Suppose now given an enumeration  $(\mathbf{x}_p)_{1 \leq p \leq 6N^2+2}$  of these points on the Cubed Sphere. To this enumeration, corresponds the application

$$(11) \quad (i, j, k) \in \left[-\frac{N}{2}, \frac{N}{2}\right] \times \left[-\frac{N}{2}, \frac{N}{2}\right] \times [(I), \dots, (VI)] \mapsto \mathbf{p}(i, j, k)$$

such that

$$(12) \quad \mathbf{x}_{\mathbf{p}(i,j,k)} = \mathbf{s}_{i,j}^k.$$

These points will serve as quadrature nodes of the two rules  $Q_a$  and  $Q_b$  introduced hereafter.

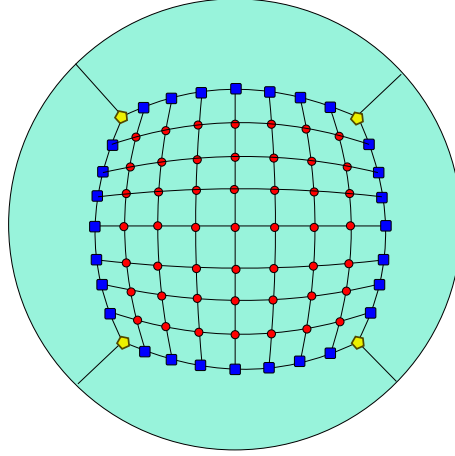


FIGURE 3. A typical panel of the Cubed Sphere: the  $(N + 1)^2$  points are classified in three categories: (i) Circles correspond to the  $(N - 1)^2$  *internal* points; (ii) Squares correspond to  $4(N - 1)$  *edge* points ; (iii) Pentagons correspond to the 4 *corner* points.

### 3. A FIRST QUADRATURE RULE

3.1. **Derivation of the rule  $Q_a$ .** In this section our first quadrature rule, called  $Q_a$ , is introduced. The quadrature nodes  $\mathbf{x}_p$  in (1) are the  $6N^2 + 2$  points  $\mathbf{s}_{i,j}^k$  defined in (10). Let  $f : \mathbb{S}^2 \mapsto \mathbb{R}$  be a regular function defined on  $\mathbb{S}^2$ . Using the decomposition

$$(13) \quad \mathbb{S}^2 = \bigsqcup_{k=(I)}^{(VI)} \mathcal{P}_k$$

allows to express  $I(f)$  as

$$(14) \quad \begin{aligned} I(f) &= \int_{\mathbb{S}^2} f(\mathbf{x}) d\sigma(\mathbf{x}) \\ &= \sum_{k=(I)}^{(VI)} \underbrace{\int_{\mathcal{P}^k} f(\mathbf{x}) d\sigma(\mathbf{x})}_{I_k(f)}. \end{aligned}$$

Defining on panel  $\mathcal{P}^k$  the change of variables  $\mathbf{x} = \varphi_k(\xi, \eta)$  gives by the chain rule,

$$(15) \quad I_k(f) = \int_{(\xi, \eta) \in [-\frac{\pi}{4}, \frac{\pi}{4}]^2} (f \circ \varphi_k)(\xi, \eta) \sqrt{|\det G(\xi, \eta)|} d\xi d\eta.$$

We denote

$$(16) \quad f_k = f \circ \varphi_k.$$

Our basic quadrature rule for the integral  $I_k(f)$  is called  $Q_k(f)$ . It is defined by

$$(17) \quad Q_k(f) = \Delta\xi\Delta\eta \sum_{i,j=-N/2}^{N/2} c_{i,j} g_{i,j} f_k(\xi_i, \eta_j).$$

In (17) the geometric weights  $g_{i,j}$  are given by (see (9)):

$$(18) \quad g_{i,j} = \sqrt{|\det G(\xi_i, \eta_j)|} = \frac{(1 + \tan^2 \xi_i)(1 + \tan^2 \eta_j)}{(1 + \tan^2 \xi_i + \tan^2 \eta_j)^{3/2}}, \quad -\frac{N}{2} \leq i, j \leq \frac{N}{2}.$$

Furthermore, the coefficients  $c_{i,j}$  are defined as follows:

- The internal points  $(i, j)$  with  $-N/2 < i, j < N/2$ , displayed with circles on Fig 3 are counted with coefficient  $c_{i,j} = 1$ .
- The edge points  $(i, j)$  with  $(i, j) \in \{[\pm N/2, -N/2 + 1 : N/2 - 1]\} \sqcup \{[-N/2 + 1 : N/2 - 1, \pm N/2]\}$  are displayed with squares on Fig. 3 and are multiplied by the coefficient  $c_{i,j} = 1/2$ .
- The four corner values  $(i, j) \in \{(-N/2, -N/2), (-N/2, N/2), (N/2, -N/2), (N/2, N/2)\}$  displayed as pentagons on Fig. 3 are multiplied by the coefficient  $c_{i,j} = 1/3$ .

This convention is natural since each edge point belongs to two neighbor panels. It is therefore counted twice hence the coefficient 1/2. Similarly, each corner point is counted three times, and this gives a coefficient 1/3 at the panel level.

**Definition 3.1.** The quadrature rule  $Q_a$  is defined as the sum of the contribution  $Q_k(f)$  of each panel  $\mathcal{P}_k$ :

$$(19) \quad Q_a(f) = \sum_{k=(I)}^{(VI)} Q_k(f).$$

or alternatively

$$(20) \quad Q_a(f) = \sum_{k=(I)}^{(VI)} \sum_{i,j=-N/2}^{N/2} c_{i,j} g_{i,j}^k f(\mathbf{s}_{i,j}^k).$$

*Remark 3.2.* In one dimension, the trapezoidal rule, expressed for  $f(x)$  defined on  $I = [0, 1]$ , is given by:

$$(21) \quad \int_0^1 f(x) dx \simeq \frac{1}{N} \left( \frac{1}{2} f(0) + \sum_1^{N-1} f(i\Delta x) + \frac{1}{2} f(1) \right).$$

On the panel  $\mathcal{P}_k$ , the formula (15) can be interpreted as the tensor product of the rule (21) on  $[-\pi/4, \pi/4] \times [-\pi/4, \pi/4]$  applied to the integrand in (15) except that the coefficient 1/3 is used at the corner points, instead of 1/4.

*Remark 3.3.* Integrating the constant function  $f^0(\mathbf{x}) \equiv 1$  on a panel  $\mathcal{P}_k$ , gives 1/6 of the area of  $\mathbb{S}^2$ , i.e.  $\frac{2\pi}{3}$ . This can be expressed using (15) as

$$(22) \quad \int_{(\xi, \eta) \in [-\frac{\pi}{4}; \frac{\pi}{4}]^2} \frac{(1 + \tan^2 \xi)(1 + \tan^2 \eta)}{(1 + \tan^2 \xi + \tan^2 \eta)^{3/2}} d\xi d\eta = \frac{2\pi}{3},$$

an identity which can be verified directly. The approximation (17) of the integral (22) is independent of the panel  $k$  with value:

$$(23) \quad Q_{(I)}(f_0) = \sum_{-N/2 < i, j < N/2} \frac{(1 + \tan^2 \xi_i)(1 + \tan^2 \eta_j)}{(1 + \tan^2 \xi_i + \tan^2 \eta_j)^{3/2}} \quad (\text{internal points}) \\ + 2(1 + \tan^2 \eta_{N/2}) \sum_{-N/2 < i < N/2} \frac{1 + \tan^2 \xi_i}{(1 + \tan^2 \xi_i + \tan^2 \eta_{N/2})^{3/2}} \quad (\text{edge points}) \\ + \frac{4}{3} \frac{(1 + \tan^2 \xi_{N/2})(1 + \tan^2 \eta_{N/2})}{(1 + \tan^2 \xi_{N/2} + \tan^2 \eta_{N/2})^{3/2}} \quad (\text{corner points})$$

and the value of  $Q_a(f_0)$  in (19) is

$$(24) \quad Q_a(f_0) = 6Q_{(I)}(f_0).$$

As will be seen in Table 3,  $Q_a(f_0) \simeq \frac{2\pi}{3}$ , with fourth order accuracy with respect to  $1/N$ .

Note that contrary to most of the quadrature rule on the sphere, this approximation is not exact (see Prop. 3.1). This is because  $f_0(\mathbf{x})$  is proportional to the Spherical Harmonic  $Y_0^0(\mathbf{x})$  which is not integrated exactly. The quadrature rule  $Q_b$  introduced in Section 4 will remedy this fact.

**3.2. Symmetry property.** Spherical Harmonics are commonly used to design quadrature rules (1). In the case where nodes and/or weights have spherical symmetries, one expects some particular subset of the Spherical Harmonics to be integrated exactly. Building quadrature rules on the sphere using invariance of the nodes under a subgroup of  $\mathbb{S}\mathbb{O}_3$  has been used by several authors. An important result in this direction is Sobolev's theorem, which asserts that a necessary and sufficient condition for a quadrature rule, invariant by a subgroup  $\mathcal{G}$  of  $\mathbb{S}\mathbb{O}_3$ , to be exact up to degree  $n$  is to be exact for all  $\mathcal{G}$ -invariant Spherical Harmonics of degree  $\leq n$ , [9]. Our rules are not a direct consequence of this result and we are considering a different approach. In a first step, we determine which Spherical Harmonics are invariant under the rule  $Q_a$ . Observe that the weights  $g_{i,j}$  in (18) do not depend on the panel  $\mathcal{P}^k$ . Furthermore they satisfy the following invariance properties for  $-N/2 \leq i, j \leq N/2$ :

- Invariance by rotation of angle  $\pi/2$ :

$$(25) \quad g_{i,j} = g_{-j,i},$$

- Invariance by symmetry with respect to the first diagonal:

$$(26) \quad g_{i,j} = g_{j,i}.$$

Combining these two transformations, it is easily seen that the coefficients  $g_{i,j}$  are symmetric with respect to the second diagonal and with respect to the coordinate lines  $i = 0$  and  $j = 0$ , respectively. Otherwise stated, the following relations hold:

$$(27) \quad g_{i,j} = g_{-j,-i} = g_{-i,j} = g_{i,-j} = g_{-i,-j}, \quad -N/2 \leq i, j \leq N/2.$$

For example for  $N = 8$ , the coefficients  $g_{i,j}$  can be arranged as shown in Table 1, where the symmetry properties (25), (26) and (27) are represented with letters. For a Cubed Sphere with parameter  $N$ , the number of independent weights is  $q_N = (N + 2)(N + 4)/8$ . These weights correspond to the indices  $0 \leq j \leq i \leq N/2$ . They are represented with boldface letters in Table 1. The number of values taken by the weights thus represents asymptotically only  $1/48$  of the number of nodes. Table 2 displays typical values of the integer  $q_N$  and of the number of quadrature nodes for a series of values of  $N$ .

$$(28) \quad \begin{array}{ccccccccc} \mathbf{a} & \mathbf{b} & \mathbf{d} & \mathbf{g} & \mathbf{k} & \mathbf{g} & \mathbf{d} & \mathbf{b} & \mathbf{a} \\ \mathbf{b} & \mathbf{c} & \mathbf{e} & \mathbf{h} & \mathbf{l} & \mathbf{h} & \mathbf{e} & \mathbf{c} & \mathbf{b} \\ \mathbf{d} & \mathbf{e} & \mathbf{f} & \mathbf{i} & \mathbf{m} & \mathbf{i} & \mathbf{f} & \mathbf{e} & \mathbf{d} \\ \mathbf{g} & \mathbf{h} & \mathbf{i} & \mathbf{j} & \mathbf{n} & \mathbf{j} & \mathbf{i} & \mathbf{h} & \mathbf{g} \\ \mathbf{k} & \mathbf{l} & \mathbf{m} & \mathbf{n} & \mathbf{o} & \mathbf{n} & \mathbf{m} & \mathbf{l} & \mathbf{k} \\ \mathbf{g} & \mathbf{h} & \mathbf{i} & \mathbf{j} & \mathbf{n} & \mathbf{j} & \mathbf{i} & \mathbf{h} & \mathbf{g} \\ \mathbf{d} & \mathbf{e} & \mathbf{f} & \mathbf{i} & \mathbf{m} & \mathbf{i} & \mathbf{f} & \mathbf{e} & \mathbf{d} \\ \mathbf{b} & \mathbf{c} & \mathbf{e} & \mathbf{h} & \mathbf{l} & \mathbf{h} & \mathbf{e} & \mathbf{c} & \mathbf{b} \\ \mathbf{a} & \mathbf{b} & \mathbf{d} & \mathbf{g} & \mathbf{k} & \mathbf{g} & \mathbf{d} & \mathbf{b} & \mathbf{a} \end{array}$$

TABLE 1. Parameters of the weights  $g_{i,j}$  in a typical panel  $\mathcal{P}^k$  in the Cubed Sphere with parameter  $N = 8$ . The independent parameters are displayed in boldface. The coefficients are symmetric with respect to the grey shadowed lines. The number of independent parameters is  $q_N = (N + 2)(N + 4)/8$ . There are 15 independent parameters in this particular case.

Cubed Sphere parameter $N$	4	8	16	32	64
Number of quad. nodes in a panel $(= (N + 1)^2)$	25	81	289	1089	4225
Number of quad. nodes on $\mathbb{S}^2 (= 6N^2 + 2)$	98	386	1538	6146	24578
Number of independent weights $q_N = (N + 2)(N + 4)/8$	6	15	45	153	561

TABLE 2. Number of quadrature nodes in function of the parameter  $N$  of the Cubed Sphere.

In summary, the quadrature rule  $Q_a$  can be expressed as

$$(29) \quad Q_a(f) = \sum_{p=1}^P w_p f(\mathbf{x}_p),$$

where

- the nodes  $\mathbf{x}_p$  are the  $P = 6N^2 + 2$  points of the Cubed Sphere of parameter  $N$ .
- the weights  $w_p$  are given by

$$(30) \quad w_p = g_{i,j}$$

where the couple  $(i, j)$  is such that  $\mathbf{x}_p = \mathbf{s}_{i,j}^k$  for some panel  $k = (I), \dots, (VI)$ . Otherwise stated,  $(i, j, k)$  is some triple of indices satisfying

$$(31) \quad (i, j, k) \in \mathbf{p}^{-1}(p)$$

where  $\mathbf{p}$  is the enumerating application defined in (12).

**3.3. The 7/8 property.** Under the assumptions (25-26) on the weights, the following claim holds:

**Proposition 3.1.** *The quadrature rule  $Q_a$  in (29) is exact, independently of the parameter  $N$ , for all Spherical Harmonics  $Y_n^m(\mathbf{x})$  satisfying*

- either  $n$  odd,
- either  $n$  even and  $m \not\equiv 0 \pmod{4}$ .

*These two series represent a proportion of 7/8 of all Spherical Harmonics.*

*Remark 3.4.* One may wonder if the Spherical Harmonics of this latter category (the remaining 1/8 Spherical Harmonics) are effectively inexactly integrated by the rule  $Q_a$  for all integers  $n$  even and  $m \equiv 0 \pmod{4}$ . This question is unanswered for the moment. In fact, the function  $Y_2^0$  ( $(n, m) = (2, 0)$ ) is exactly integrated by the rule  $Q_a$ . Prop. 3.1 therefore only describes a sufficient condition for the exactness of the rule  $Q_a$ .

*Proof.* The Spherical Harmonic  $Y_n^m$  is (see (2)):

$$(32) \quad Y_n^m(\mathbf{x}) = (-1)^m N_n^{|m|} P_n^{|m|}(\sin \theta) e^{im\lambda}, \quad n \geq 0, \quad -n \leq m \leq n$$

The exact integration property stated in Prop. 3.1 is based on the fact that non zero values of  $Y_n^m(\mathbf{x})$  have their exact opposite on another part of the Cubed Sphere. This property is due to the symmetries (25, 26) of the weights  $g_{i,j}$ , and to the following relations:

$$(33) \quad Y_n^m(\lambda + \pi, \theta) = (-1)^m \times Y_n^m(\lambda, \theta),$$

$$(34) \quad Y_n^m(\lambda, -\theta) = (-1)^{n+m} \times Y_n^m(\lambda, \theta),$$

$$(35) \quad Y_n^m\left(\lambda + p\frac{\pi}{m}, \theta\right) = (-1)^p \times Y_n^m(\lambda, \theta)$$

with  $n > 0$ ,  $m \in \{-n, \dots, n\} \setminus \{0\}$ ,  $p \in \mathbb{Z}$ , and  $(\lambda, \theta) \in [-\pi, \pi) \times [-\frac{\pi}{2}, \frac{\pi}{2}]$ . Note that (33) is a particular case of (35).

We consider the four following cases. In each case, the approximate value  $Q_a(Y_n^m)$  is compared to the exact integral  $I(Y_n^m)$  in (4).

- **Case  $n$  odd.** Consider first the case where  $m$  is even, then the property (34) leads to

$$(36) \quad Q_{(I)}(Y_n^m) = Q_{(II)}(Y_n^m) = Q_{(III)}(Y_n^m) = Q_{(IV)}(Y_n^m) = 0,$$

due to opposite values of  $Y_n^m(\lambda, \theta)$  for opposite values of  $\theta$ , and to the properties  $g_{i,j} = g_{i,-j}$  of the weights. Moreover, using that the weights  $g_{i,j}$  are the same on the six panels, we have

$$(37) \quad Q_{(V)}(Y_n^m) = -Q_{(VI)}(Y_n^m).$$

This gives  $Q_a(Y_n^m) = 0$ .

Consider now the case where  $m$  is odd. Then the relation (33) leads to the relations

$$(38) \quad Q_{(I)}(Y_n^m) = -Q_{(III)}(Y_n^m), \quad Q_{(II)}(Y_n^m) = -Q_{(IV)}(Y_n^m).$$

We have used the relation  $g_{i,j} = g_{-i,j}$  and the fact that the weights  $g_{i,j}$  are identical on each panel. Furthermore due to (33) and  $g_{i,j} = g_{-i,-j}$  (symmetry of the weights with respect to the center of each panel) we find

$$(39) \quad Q_{(V)}(Y_n^m) = Q_{(VI)}(Y_n^m) = 0.$$

Summing up over the six panels yields  $Q_a(Y_n^m) = 0$  (exact value).

- **Case  $n$  even and  $m$  odd.** In this case,  $n + m$  is odd, and then (34) shows that  $Q_k(Y_n^m) = 0$  for the panels  $k = (I), (II), (III)$  and  $(IV)$ . This is due to the fact that the weights  $g_{i,j}$  have the property  $g_{i,j} = g_{i,-j}$ . For the panels  $k = (V)$  and  $k = (VI)$ , we have  $Q_k(Y_n^m) = 0$  due to (33) and  $g_{i,j} = g_{-i,-j}$ . Therefore  $Q_a(Y_n^m) = 0$ .
- **Case  $n$  even,  $m$  even and  $m \not\equiv 0 \pmod{4}$ .** In this case,  $Q_k(Y_n^m) = 0$  for the panels  $k = (V)$  and  $k = (VI)$ . This is due to (35) (take  $p = \frac{m}{2}$  in this formula) and to the fact that the weights  $g_{i,j}$  satisfy (25). Moreover, again using (35) with  $p = \frac{m}{2}$ , one has  $Q_{(I)}(Y_n^m) = -Q_{(II)}(Y_n^m)$  and  $Q_{(III)}(Y_n^m) = -Q_{(IV)}(Y_n^m)$ . Note in addition that  $Q_{(I)}(Y_n^m) = Q_{(III)}(Y_n^m)$ . This yields  $Q_a(Y_n^m) = 0$ .

• **Case  $n$  even,  $m$  even and  $m \equiv 0 \pmod{4}$ .** Note that the constant function  $Y_0^0 \equiv 1/\sqrt{4\pi}$  belongs to this category. In this case,

$$(40) \quad Q_{(I)}(Y_n^m) = Q_{(II)}(Y_n^m) = Q_{(III)}(Y_n^m) = Q_{(IV)}(Y_n^m).$$

This is due to the property (35). In addition, due to (34),

$$(41) \quad Q_{(V)}(Y_n^m) = Q_{(VI)}(Y_n^m),$$

In this case, a possible cancellation between the terms of the approximate integral  $Q_a(Y_n^m)$  could only occur between the contribution of panels (I), (II), (III) and (IV) on the one hand and the contribution of panels (V) and (VI) on the other hand. Such a cancellation does not occur in general. This explains why  $Q_a(Y_n^m)$  is not exact in general in this case.

Clearly, the three first cases describe all together a proportion of (asymptotically) 7/8 of all Spherical Harmonics. The latter case corresponds to the remaining 1/8 Spherical Harmonics.  $\square$

**3.4. Numerical results.** In this section we show numerical results obtained with the rule  $Q_a$ . The functions  $f_0, f_1, f_2, f_3$  and  $f_4$  that are used to test numerical quadrature formula are [8, 4]:

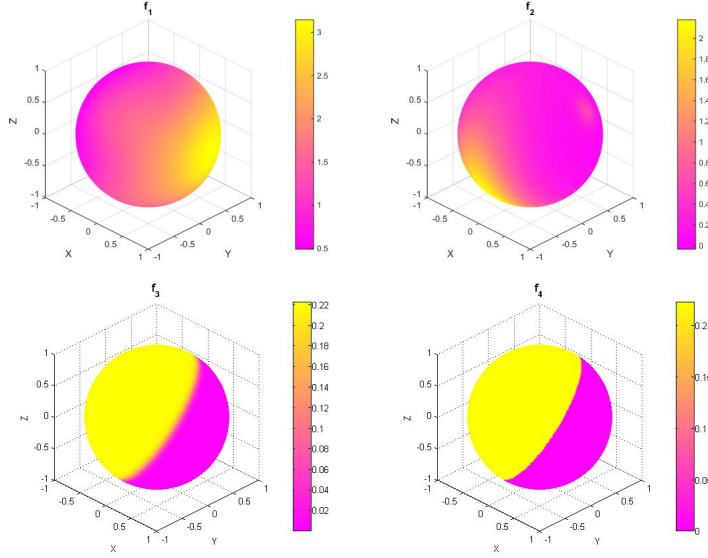
$$(42) \quad \left\{ \begin{array}{l} f_0(x, y, z) \equiv 1, \\ f_1(x, y, z) = 1 + x + y^2 + x^2y + x^4 + y^5 + x^2y^2z^2, \\ f_2(x, y, z) = 0.75e^{-(9x-2)^2/4-(9y-2)^2/4-(9z-2)^2/4} \\ \quad + 0.75e^{-(9x+1)^2/49-(9y+1)/10-(9z+1)/10} \\ \quad + 0.5e^{-(9x-7)^2/4-(9y-3)^3/4-(9z-5)^2/4} \\ \quad - 0.2e^{-(9x-4)^2-(9y-7)^2-(9z-5)^2}, \\ f_3(x, y, z) = (1 + \tanh(-9x - 9y + 9z))/9, \\ f_4(x, y, z) = (1 + \text{sign}(-9x - 9y + 9z))/9. \end{array} \right.$$

The exact values are given by:

$$(43) \quad \left\{ \begin{array}{l} \int_{\mathbb{S}^2} f_0 = 4\pi \\ \int_{\mathbb{S}^2} f_1 = \frac{216\pi}{35}, \\ \int_{\mathbb{S}^2} f_2 = 6.6961822200736179523\dots, \\ \int_{\mathbb{S}^2} f_3 = \frac{4\pi}{9}, \\ \int_{\mathbb{S}^2} f_4 = \frac{4\pi}{9}. \end{array} \right.$$

The functions  $f_1, f_2, f_3$  and  $f_4$  are represented on Fig. 4.

The function  $f_1$  is a polynomial function of degree 6. Its expansion in Spherical Harmonics  $Y_n^m$  therefore involves values of  $n \leq 6$ . One expects an excellent accuracy of any spherical quadrature rule for this function. In the contrary,  $f_2, f_3$  and  $f_4$  have an infinite Spherical Harmonics expansion. The function  $f_2$  is smooth whereas  $f_3$  has sharp gradients. The function  $f_4$  is a limiting case of  $f_3$  and is discontinuous. The numerical results for several values of the Cubed Sphere parameter  $N$  are displayed in Table 3. The total number of nodes on  $\mathbb{S}^2$  is given in each case. Following [8], we

FIGURE 4. The set of test functions  $f_1$ ,  $f_2$ ,  $f_3$  and  $f_4$ .

display the accuracy for the test functions in (42), by retaining the worst case among 1000 random solid rotations operated on the argument  $(x, y, z)$  of the function. The results for  $f_4$  are identical to the results for  $f_3$  and are therefore not reported. A fourth order convergence rate is observed on Fig. 5. The accuracy is very good, compared to results reported elsewhere. For example, for a

$N$	Number of nodes	$ I(f_0) - Q_a(f_0) $	$ I(f_1) - Q_a(f_1) $	$ I(f_2) - Q_a(f_2) $	$ I(f_3) - Q_a(f_3) $
4	98	1.0023(-2)	1.623(-2)	1.721(-2)	1.114(-3)
6	218	1.9528(-3)	2.900(-3)	2.638(-3)	2.170(-4)
8	386	6.1462(-4)	9.849(-4)	8.320(-4)	6.829(-5)
10	602	2.5111(-4)	4.008(-4)	2.157(-4)	2.790(-5)
12	866	1.2093(-4)	1.900(-4)	7.791(-5)	1.344(-5)
14	1178	6.5219(-5)	1.017(-4)	3.810(-5)	7.247(-6)
16	1538	3.8209(-5)	5.828(-5)	2.080(-5)	4.245(-6)
32	6146	2.3848(-6)	3.747(-6)	1.339(-6)	2.650(-7)
64	24578	1.4900(-7)	2.258(-7)	8.089(-8)	1.656(-8)

TABLE 3. Accuracy of the quadrature rule  $Q_a$  for the test functions  $f_0$ ,  $f_1$ ,  $f_2$  and  $f_3$  in (42). The errors for  $f_4$  are identical to the errors for  $f_3$ . The result corresponds to the worst case among 1000 randomly selected solid rotations operated on the argument  $(x, y, z)$  of the functions  $f_1$ ,  $f_2$ ,  $f_3$ .

Cubed Sphere with parameter  $N \leq 12$ , corresponding to  $6N^2 + 2 \leq 1000$  quadrature nodes on the sphere, the accuracy is of the same order as the one obtained with optimally selected quadrature nodes [8].

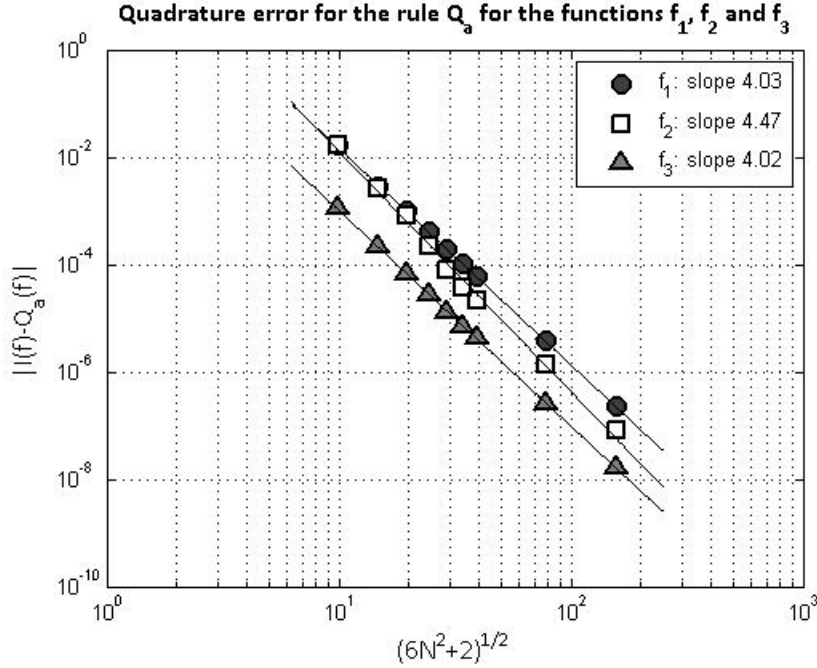


FIGURE 5. Quadrature error for the test functions  $f_1$ ,  $f_2$  and  $f_3$  obtained with rule  $Q_a$  in function of the square root of the number of quadrature nodes on the sphere ( $6N^2 + 2$  nodes). The accuracy is indicated for each function. Fourth-order accuracy based on regression lines is observed in the three cases. The worst case among 1000 randomly selected solid rotations on the argument  $(x, y, z)$  of the functions is displayed. The results for  $f_4$  are identical to the ones of  $f_3$ . The slope for the constant function  $f_0$  is 4.01 (not shown).

*Remark 3.5.* A proof of the fourth order accuracy of the rule  $Q_a$  is not straightforward. In particular, it cannot be simply deduced from the accuracy of the trapezoidal rule in one dimension, since the rule  $Q_a$  is not exactly a tensor product rule on each panel, see Remark 3.2.

#### 4. A SECOND QUADRATURE RULE

**4.1. Derivation of the rule  $Q_b$ .** As shown in Prop. 3.1, the quadrature rule  $Q_a$  in (19) is exact for a proportion of 7/8 of all Spherical Harmonics. However, it is in general not exact for the remaining 1/8 Spherical Harmonics. In this latter case, it is numerically observed to be fourth-order accurate with respect to the parameter  $1/N$ , (see Fig. 5 and Remarks 3.4 and 3.5). This fact suggests to look for a new rule  $Q_b$  such that:

- it keeps the 7/8 exactness property
- it has a better accuracy than  $Q_a$  for the 1/8 remaining Spherical Harmonics.

In order to do this, the idea is to design the rule  $Q_b$  as a perturbation of  $Q_a$  in the following way:

- (1) The rule  $Q_b$  keeps the same structure than  $Q_a$  i.e.:

$$(44) \quad Q_b(f) = \sum_{k=(I)}^{(VI)} \hat{Q}_k(f),$$

(2) The contribution of the panel  $\mathcal{P}^k$  is

$$(45) \quad \widehat{Q}_k(f) = \Delta\xi\Delta\eta \sum_{i,j=-N/2}^{N/2} c_{i,j} \widehat{g}_{i,j} f_k(\xi_i, \eta_j)$$

where the weight  $\widehat{g}_{i,j}$  is a perturbation of of the geometric weight  $g_{i,j}$  of the form:

$$(46) \quad \widehat{g}_{ij} = g_{i,j} + \varepsilon_{i,j}.$$

It results from (44,45) that the rule  $Q_b$  can be expressed as:

$$(47) \quad Q_b(f) = Q_a(f) + \Delta\xi\Delta\eta \sum_{k=(I)}^{(VI)} \sum_{i,j=-N/2}^{N/2} c_{i,j} \varepsilon_{i,j} f_k(\xi_i, \eta_j).$$

If the values  $\varepsilon_{i,j}$  satisfy the symmetries (25) and (26) then by Prop. 3.1, the rule  $Q_b$  satisfies the 7/8 property as well.

Let us call  $\mathcal{I}$  the set of indices  $(i,j)$  such that  $0 \leq j \leq i \leq N/2$ . This set is represented in Table 1 by boldface letters. Recall that  $|\mathcal{I}| = q_N = (N+2)(N+4)/8$ . The term  $Q_k(f)$  in (17) can be expressed as

$$(48) \quad Q_k(f) = \Delta\xi\Delta\eta \sum_{(i,j) \in \mathcal{I}} g_{i,j} \widehat{f}_{i,j}^k.$$

where  $\widehat{f}_{i,j}^k$  denotes, for  $(i,j) \in \mathcal{I}$  and  $(I) \leq k \leq (VI)$ , (recall that  $f_k = f \circ \varphi_k$ , see (15-17)):

$$(49) \quad \widehat{f}_{i,j}^k = c_{i,j} \sum_{(i',j') | g_{i',j'} = g_{i,j}} f_k(\xi_{i'}, \eta_{j'}).$$

With this notation, (45) can be expressed as

$$(50) \quad Q_k(f) = \Delta\xi\Delta\eta \sum_{(i,j) \in \mathcal{I}} (g_{i,j} + \varepsilon_{i,j}) \widehat{f}_{i,j}^k.$$

**4.2. Determining the weights  $\varepsilon_{i,j}$ .** Now we need to evaluate suitable values of the  $q_N$  unknowns  $(\varepsilon_{i,j})_{(i,j) \in \mathcal{I}}$ . Let us denote by

$$(51) \quad \psi_1 = Y_0^0, \quad \psi_2 = Y_2^0, \quad \psi_3 = Y_4^0, \quad \psi_4 = Y_4^4, \dots$$

the sequence of the Spherical Harmonics  $Y_n^m$  with  $n$  even and  $m \geq 0$ ,  $m \equiv 0 \pmod{4}$ . This is the sequence of the 1/8 of all Spherical Harmonics possibly not exactly integrated by the rule  $Q_a$  (see Prop 3.1).

Let us define the set of equations for the values  $\varepsilon_{i,j}$  as

$$(52) \quad Q_b(\psi_l) = I(\psi_l), \quad 1 \leq l \leq p_N.$$

The integer  $p_N$ , to be determined, is the number of Spherical Harmonics of the preceding form taken in account in (52). This is a parameter of the rule  $Q_b$ . Using (47), equation (52) is recast in the form:

$$(53) \quad \sum_{(i,j) \in \mathcal{I}} \left( \Delta\xi\Delta\eta \sum_{k=(I)}^{(VI)} (\widehat{\psi}_l)_{i,j}^k \right) \varepsilon_{i,j} = I(\psi_l) - Q_a(\psi_l), \quad 1 \leq l \leq p_N.$$

**Lemma 4.1.** For each  $l \leq 0$ ,  $(I) \leq k \leq (VI)$  and  $(i, j) \in \mathcal{I}$ ,

$$(54) \quad I(\psi_l) - Q_a(\psi_l) \in \mathbb{R}$$

and

$$(55) \quad (\widehat{\psi}_l)_{i,j}^k \in \mathbb{R}.$$

*Proof.* Let  $\psi_l = Y_n^m$  with  $n = 2n'$ ,  $m = 4m'$ ,  $0 \leq m \leq n$ . The imaginary part of  $Y_n^m(\mathbf{x})$  is called  $H_n^m(\mathbf{x})$ . According to (2),  $H_n^m(\mathbf{x})$  is expressed as

$$(56) \quad H_n^m(\lambda, \theta) = N_n^m P_n^m(\sin \theta) \sin(m\lambda).$$

The imparity with respect to the longitude variable  $\lambda$  gives

$$(57) \quad H_n^m(-\lambda, \theta) = -H_n^m(\lambda, \theta).$$

The relation  $g_{-i,j} = g_{i,j}$  combined with (57) implies that the discrete integral of  $H_n^m$  on the panel  $\mathcal{P}^{(k)}$  with  $k = (I)$  is

$$(58) \quad Q_k(H_n^m) = 0.$$

Furthermore the relation (35) with  $p = \pm 2m'$ ,  $m = 4m'$  gives the relation (58) on the two panels  $k = (II)$  and  $k = (IV)$ . Next, (33) yields (58) for the panel  $k = (III)$ . Consider now the panel  $k = (V)$ . The value  $Q_{(V)}(H_n^m)$  can be decomposed in four terms each of them corresponding to an angular sector, see (16):

$$(59) \quad \begin{aligned} Q_{(V)}(H_n^m) &= \sum_{i,j=-N/2}^{N/2} c_{i,j} g_{i,j} [H_n^m]_{(V)}(\xi_i, \eta_j) \\ &= \sum_{(i,j) | j < -|i|} c_{i,j} g_{i,j} [H_n^m]_{(V)}(\xi_i, \eta_j) + \sum_{(i,j) | i \geq |j|} c_{i,j} g_{i,j} [H_n^m]_{(V)}(\xi_i, \eta_j) \\ &\quad + \sum_{(i,j) | j \geq |i|} c_{i,j} g_{i,j} [H_n^m]_{(V)}(\xi_i, \eta_j) + \sum_{(i,j) | i < -|j|} c_{i,j} g_{i,j} [H_n^m]_{(V)}(\xi_i, \eta_j). \end{aligned}$$

In the right hand side of (59), the first term vanishes, due to (57) and the relation  $g_{-i,j} = g_{i,j}$ . The relations (34) and (35) imply that the three other terms also vanish. The argument is similar for the panel  $k = (VI)$ . A similar argument shows that the imaginary part of  $(\widehat{\psi}_l)_{i,j}^k \in \mathbb{R}$  for all  $l \geq 0$ ,  $(i, j) \in \mathcal{I}$  and  $(I) \leq k \leq (VI)$  also vanish. Therefore  $Q_a(\psi_l) \in \mathbb{R}$  and since  $I(\psi_l) \in \mathbb{R}$ , the relation (54) holds.  $\square$

The set of relations (53) forms a real linear system

$$(60) \quad A\boldsymbol{\varepsilon} = \mathbf{b},$$

with unknown vector

$$(61) \quad \boldsymbol{\varepsilon} = (\varepsilon_{i,j})_{(i,j) \in \mathcal{I}} \in \mathbb{R}^{q_N}.$$

As mentioned above, the number  $p_N$  of Spherical Harmonics  $Y_n^m$  with  $n$  even and  $m \equiv 0 \pmod{4}$  to be taken in account in (52) has to be determined.

In the following we have selected the value  $p_N = N^2/4$ . This value was obtained by plotting the quadrature errors  $|I(f) - Q_b(f)|$  for the functions  $f_1$ ,  $f_2$  and  $f_3$  against the number  $p_N$  of Spherical Harmonics taken in account in the linear system (60). Three typical plots corresponding to  $N = 4, 8$  and  $16$  are shown on Fig. 6. A highly accurate zone is located on the left part of each plot. Then a loss of accuracy, more or less abrupt, can be observed when  $p_N$  becomes large. In view of these results we have selected the value  $p_N = N^2/4$  as a compromise for high accuracy of

the rule. The location of  $p_N = N^2/4$  is reported on these plots. This value is selected in order to be located "well within" the highly accurate portion of the rule  $Q_b$ . With this choice, the matrix  $A$  in (60) is rectangular with

$$(62) \quad A \in \mathbb{M}_{p_N, q_N}(\mathbb{R}), \quad p_N = N^2/4, \quad q_N = (N+2)(N+4)/8.$$

For  $N \geq 8$ ,  $p_N = N^2/4 > q_N \simeq N^2/8$ , and thus the system (60) is overdetermined. We solve (60) using the pseudo-inverse of Moore-Penrose [7, Chap. 3, pp. 57sq]. We have used the *matlab* routine *pinv*.

*Remark 4.2.* Since the pseudo-inverse is used to solve the rectangular system (60), the identity (52) for the Spherical Harmonic  $\psi_l$ ,  $1 \leq l \leq p_N$  is not exactly satisfied, but only approximately. Therefore, strictly speaking, the rule  $Q_b$  does not integrate all Spherical Harmonics up to a certain order. In particular, there is no meaning for the McLaren index [13], reporting the ratio of the maximal degree of Spherical Harmonics exactly integrated to the number of quadrature nodes. Despite this observation, the rule  $Q_b$  was observed to be highly accurate on the numerical tests performed so far.

*Remark 4.3.* The function  $Y_2^0$  corresponds to  $(n, m) = (2, 0)$ , ( $n$  even and  $m \equiv 0 \pmod{4}$ ). Thus it belongs to the  $1/8$  complementary set of Spherical Harmonics in Prop. 3.1. However, as mentioned in Remark 3.4,  $Y_2^0$  is exactly integrated by the rule  $Q_a$ . Therefore  $Y_2^0$  could be taken out from the set of functions  $\psi_l$  in (52). The function  $Y_2^0$  corresponds to a null line in (60). Keeping it does not prevent the generalized inverse to be used to solve the linear system (60).

*Remark 4.4.* An important question is whether or not the matrix  $A$  in (60) is full rank. This problem is open for the moment. Preliminary numerical experiments suggest that the matrix  $A$  may be not full rank for small values of the parameter  $N$ , which means for a coarse Cubed Sphere ( $N \leq 12$ ), and becomes full rank for larger values of  $N$ . This question requires further theoretical and numerical investigation. In our numerical experiments, we never observed numerical ill conditioning effects of the matrix  $A$  when solving the linear system (60).

**4.3. Magnitude of the parameters  $\varepsilon_{i,j}$ .** In Section 4.1, we claimed that the perturbation weights  $\varepsilon_{i,j}$  are small perturbation of the geometric weights  $g_{i,j}$ . We report in Fig. 7, the magnitude of the coefficients  $\varepsilon_{i,j} \in \mathbb{R}$ , solution of the equation (60). This magnitude is numerically evaluated as  $\max_{i,j} |\varepsilon_{i,j}|$ . Clearly this maximum is small, with respect to the metric tensor terms  $g_{i,j}$ , which satisfies  $g_{i,j} \in [0.5, 1]$ , see (18). In fact, as shown in Fig. 7, the maximum of  $|\varepsilon_{i,j}|$  decreases in  $O\left(\frac{1}{N^2}\right)$  when  $N$  increases. This suggests that the rule  $Q_b$  can be effectively considered as a perturbation of the rule  $Q_a$ .

**4.4. Efficiency of the rule  $Q_b$ .** In this section, we numerically evaluate the efficiency of the rule  $Q_b$  on several Spherical Harmonics. Since the rule  $Q_b$  possesses the  $7/8$  property, (see Prop. 3.1), we consider how  $Q_b$  behaves when approximately integrating any given Spherical Harmonic  $Y_{n_0}^{m_0}$  with  $n_0$  even and  $m_0 \equiv 0 \pmod{4}$ . On Fig. 8 three typical cases are displayed:  $(n_0, m_0) = (16, 8)$ ,  $(n_0, m_0) = (24, 4)$ , and  $(n_0, m_0) = (40, 16)$ . As can be observed in these three cases, there is an abrupt enhancement of the accuracy of the rule  $Q_b$  for some threshold value of the number of quadrature nodes. At this threshold value, the function  $Y_{n_0}^{m_0}$  becomes included in the set of Spherical harmonics defining (60) and the approximation  $I(Y_{n_0}^{m_0}) \simeq Q_b(Y_{n_0}^{m_0})$  holds up to computer accuracy. Note that this behaviour occurs despite the fact that the linear system (60) is only approximately satisfied by the least square solution  $\varepsilon$ . These observations have been confirmed in other cases.

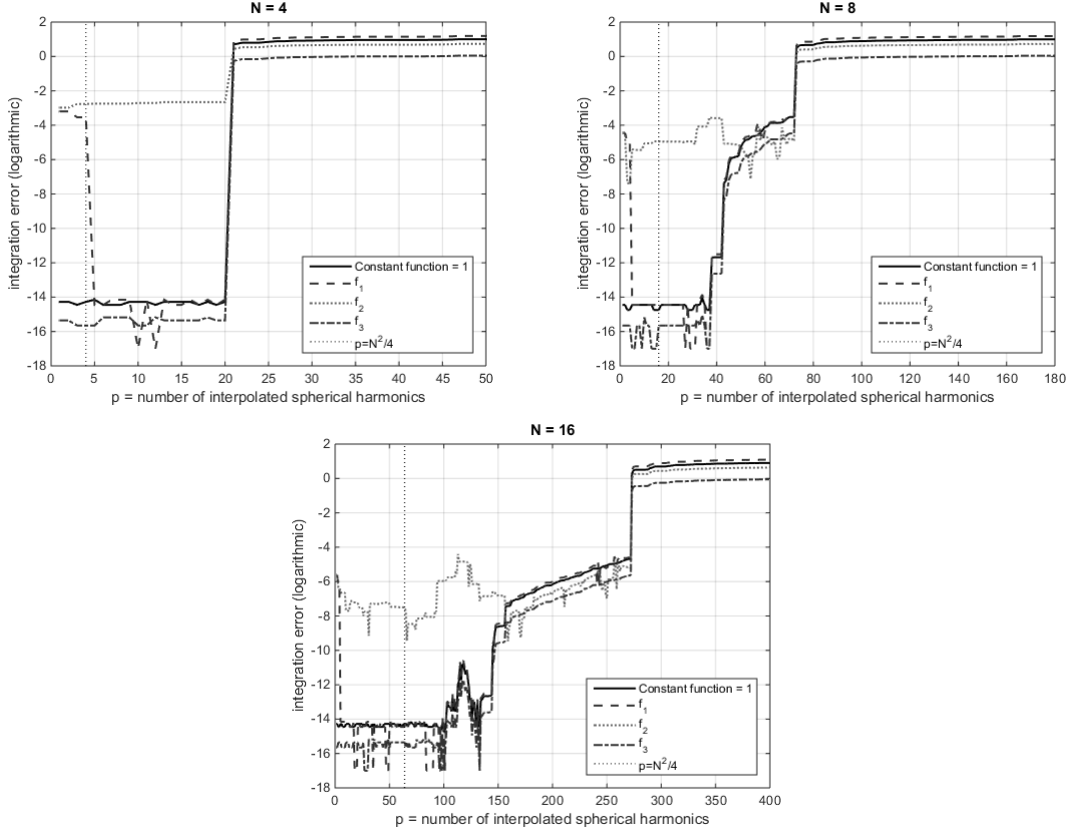


FIGURE 6. Quadrature error for the test functions  $f_1$ ,  $f_2$  and  $f_3$  in function of the number  $p_N$  of the Spherical Harmonics taken in account in (52) defining the rule  $Q_b$ . The retained value  $p_N = N^2/4$  is indicated with a dashed line.

Our numerical experiments can be summarized as follows. The rules  $Q_a$  and  $Q_b$  give similar results for the Spherical Harmonics not taken in account in the interpolation in (53), (or equivalently, in the matrix  $A$  in (60)). This indicates that the rule  $Q_b$  preserves the good convergence properties of the rule  $Q_a$  when  $N$  increases for all the functions  $Y_n^m$  with  $n \geq n_0$ , where  $n_0$  is any fixed value. Furthermore, the rule  $Q_b$  integrates up to computer accuracy a Spherical Harmonic  $Y_n^m$  from the moment it is taken in account in the linear system (53) for the perturbation weights  $\varepsilon$ . Finally, the greater is  $N$ , the more Spherical Harmonics can be taken in account in the matrix  $A$ .

**4.5. Numerical results.** In Table 4, numerical results obtained with the rule  $Q_b$  (44) applied to the set of test functions (42) are reported. As in Table 3, the worst case among 1000 randomly selected solid rotations is retained. According to results displayed in Table 4 and Fig. 9, the quadrature rule  $Q_b$  is much more accurate than the rule  $Q_a$ . Indeed, for a very coarse Cubed Sphere with parameter  $N \simeq 6$ , the computer accuracy is reached ( $\simeq 10^{-15}$ ) for the functions  $f_1$ ,  $f_3$  and  $f_4$ . This accuracy can be explained as follows. Since  $f_1$  is a polynomial, only the first Spherical Harmonics are useful, and therefore when the parameter  $p_N$  is such that  $p_N \geq 9$ , all Spherical Harmonics in the decomposition of  $f_1$  are integrated exactly by the rule  $Q_b$ . The functions  $f_3$  and

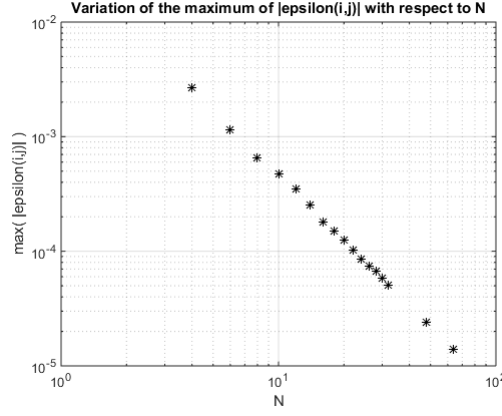


FIGURE 7. Maximum of the parameters  $|\varepsilon_{i,j}|$  in (60) with respect to  $N$ , the parameter of the Cubed Sphere. The values of  $N$  are the 17 values  $N = 4, 6, 8, \dots, 28, 30, 32, 48, 64$ . The magnitude of  $(\varepsilon_{i,j})_{(i,j) \in \mathcal{I}}$  behaves numerically as  $1/N^2$ .

$N$	Number of nodes	$p_N$	$ I(f_0) - Q_b(f_0) $	$ I(f_1) - Q_b(f_1) $	$ I(f_2) - Q_b(f_2) $	$ I(f_3) - Q_b(f_3) $
4	98	4	3.553(-15)	1.646(-4)	1.376(-2)	6.661(-16)
6	218	9	5.329(-15)	7.105(-15)	2.664(-3)	6.661(-16)
8	386	16	1.776(-15)	3.553(-15)	8.085(-4)	4.441(-16)
10	602	25	5.329(-15)	1.066(-14)	1.067(-4)	6.661(-16)
12	866	36	1.776(-15)	3.553(-15)	1.270(-5)	2.220(-16)
14	1178	49	1.776(-15)	3.553(-15)	1.272(-6)	4.441(-16)
16	1538	64	1.776(-15)	1.066(-14)	8.212(-8)	6.661(-16)
32	6146	256	3.553(-15)	7.105(-15)	3.610(-13)	6.661(-16)
64	24578	1024	3.553(-15)	7.105(-15)	2.000(-15)	4.441(-16)

TABLE 4. Accuracy of the quadrature rule  $Q_b$  for the test functions  $f_1$ ,  $f_2$  and  $f_3$  in (42). The computer accuracy is reached from a number of quadrature nodes as low as 218 for the functions  $f_1$  and  $f_3$ . The results correspond to the worst case among 1000 randomly selected solid rotations applied to the arguments  $(x, y, z)$  of the functions  $f_1$ ,  $f_2$  and  $f_3$ .

$f_4$  illustrate the accuracy of the rule  $Q_b$ , which is due to the symmetry properties (25), (26) and (27) combined with the good integration of  $Y_0^0$ . As mentioned in [4], the Spherical Harmonics in the decomposition of  $f_3$  are limited to  $Y_0^0$  and  $Y_n^m$  with  $n$  odd. Thus it is sufficient for a rule to integrate exactly  $Y_0^0$  since the Spherical Harmonics with an odd degree are exactly integrated thanks to the 7/8 property. The same observation holds for  $f_4$ . Consequently, from the moment that  $p_N \geq 1$ , the rule  $Q_b$  already gives much better results than the rule  $Q_a$  simply because  $Y_0^0$  is the first Spherical Harmonic taken in account in the matrix  $A$  in (60).

In the case of  $f_2$ , the improvement is less dramatic. This is because there are Spherical Harmonics in the decomposition of  $f_2$ , which are not taken in account in the matrix  $A$  in (60). Therefore the

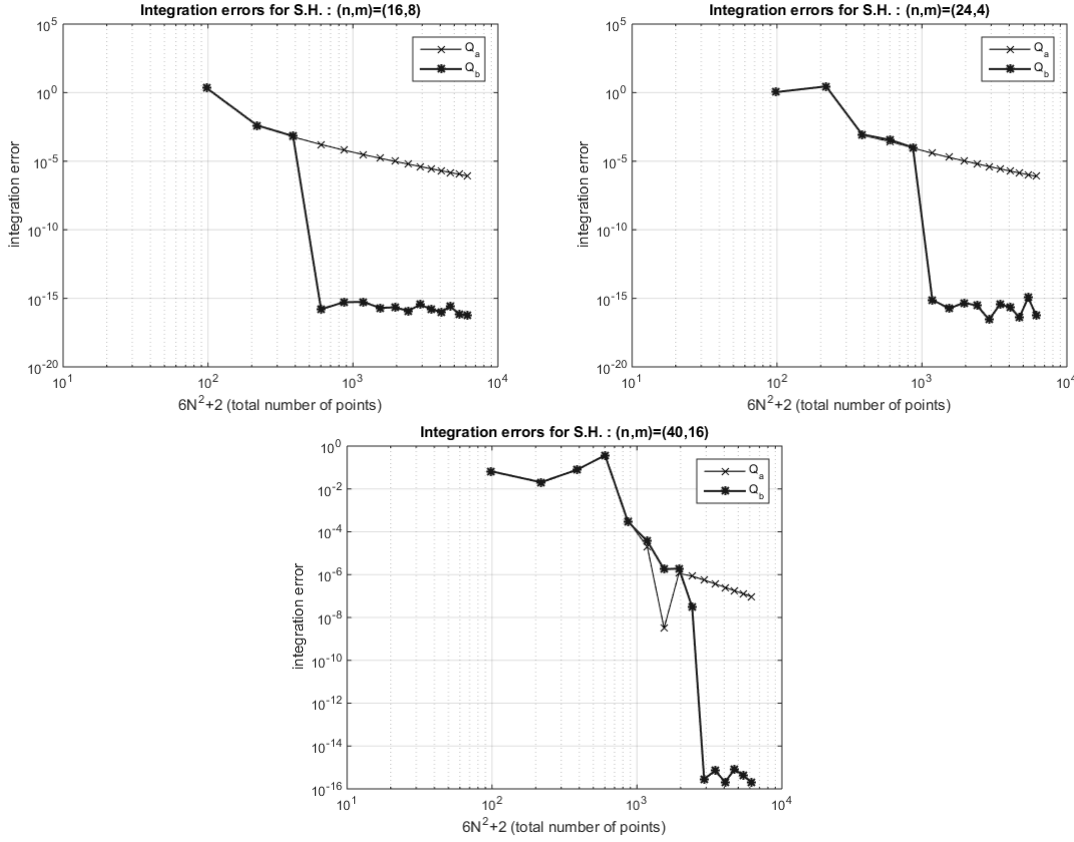


FIGURE 8. The three figures display the integration errors in function of  $N$ , the parameter of the Cubed Sphere, for the three Spherical Harmonics  $Y_{16}^8$ ,  $Y_{24}^4$  and  $Y_{42}^{16}$ . The Log scale is used along  $x$  and  $y$ . The thin curve with  $\times$  symbols corresponds to the rule  $Q_a$ . The bold curve with  $*$  symbols corresponds to the rule  $Q_b$ . Observe on the third plot a punctual better accuracy of  $Q_a(Y_{42}^{16})$  than of  $Q_b(Y_{42}^{16})$  for the particular value  $N = 16$ . This is a superconvergence phenomenon of  $Q_a$  in this case.

error decreases progressively. However the decreasing rate is very fast: the slope shown in Fig. 9 is numerically evaluated as close to 12, instead of 4 for the rule  $Q_a$  (see Fig. 5). Overall, as observed in Table 4, the level of accuracy obtained with  $Q_b$  is very good when compared with quadrature rules using optimally selected set of nodes, [8].

### 5. CONCLUSION

In this paper, we have considered a method to build quadrature rules over the sphere with the Cubed Sphere gridpoints as quadrature nodes. The symmetry of this set of nodes gives the property that when combined with a suitably chosen set of weights, a ratio of 7/8 of all Spherical Harmonics are exactly integrated, independently of the size of the Cubed Sphere. Two rules of this kind are introduced. The first rule  $Q_a$  is an analog of the trapezoidal rule on the sphere. The second rule  $Q_b$ , is an enhancement of the rule  $Q_a$ , and provides very good accuracy on a standard

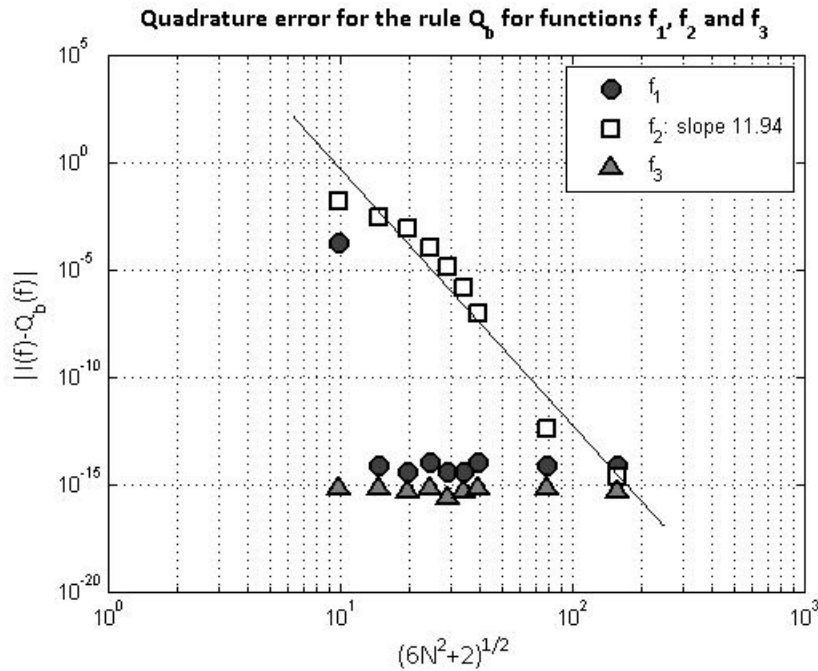


FIGURE 9. Quadrature error for the test functions  $f_1$ ,  $f_2$  and  $f_3$  obtained with the rule  $Q_b$  in function of the square root of the number  $6N^2 + 2$  of quadrature nodes on the sphere. The results for  $f_4$  are identical to the results for  $f_3$ . The computer accuracy is obtained for all grids for  $f_0$  (not reported). The convergence rate obtained by the regression line is close to 12 for the function  $f_2$ .

set of test functions. It is observed to be efficient not only when applied to regular functions, but also when applied to discontinuous functions such as  $f_4$  in (42).

Ongoing studies focus on the one hand on mathematical properties and numerical analysis of the rules  $Q_a$  and  $Q_b$ . On the other hand, a systematic approach for the logic of the design of the rule  $Q_b$  as a perturbation of  $Q_a$  is needed. This concerns in particular the choice of the functions  $\psi_l$  in the relation (52).

#### ACKNOWLEDGEMENT

The authors thank the reviewers for the careful rereading. This greatly helped to enhance this work.

#### REFERENCES

- [1] C. Ahrens and G. Beylkin. Rotationally invariant quadratures for the sphere. *Proceedings of the Royal Society of London A*, 465(2110):3103–3125, 2009.
- [2] K. Atkinson and W. Han. *Spherical Harmonics and Approximations on the Unit Sphere: an introduction*. Number 2044 in Lect. Notes. Math. Springer-Verlag, 2012.
- [3] L. Bao, R. D. Nair, and H. M. Tufo. A mass and momentum flux-form high-order discontinuous Galerkin shallow water model on the Cubed-Sphere. *J. Comput. Phys.*, 271:224–243, 2014.
- [4] C. H. L. Beentjes. Quadrature on a spherical surface. Working note available on the website <http://people.maths.ox.ac.uk/beentjes/Essays/>, 2015.

- [5] J.-P. Croisille. Hermitian compact interpolation on the Cubed-Sphere grid. *Jour. Sci. Comp.*, 57,1:193–212, 2013.
- [6] J.-P. Croisille. Hermitian approximation of the spherical divergence on the Cubed-Sphere. *Jour. Comp. App. Math.*, 280:188–201, 2015.
- [7] P. Deuffhard and A. Hohmann. *Numerical Analysis in Modern Scientific Computing. An Introduction*. Number 43 in TAM. Springer-Verlag, 2cd edition, 2003.
- [8] B. Fornberg and J.M. Martel. On spherical harmonics based numerical quadrature over the surface of a sphere. *Adv. Comp. Math.*, 40(5-6):1169–1184, 2014.
- [9] K. Hesse, I.H. Sloan, and R. S. Womersley. Chap. 40: Numerical Integration on the Sphere. In W. Freeden, M. Z. Nashed, and T. Sonar, editors, *Handbook of Geomathematics*. Springer, 2010.
- [10] M. N. Jones. *Spherical Harmonics and Tensors for classical field theory*. Research Studies Press, 1985.
- [11] J. Keiner and D. Potts. Fast evaluation of quadrature formulae on the sphere. *Math. Comp.*, 77(261):397–419, 2008.
- [12] P. Lauritzen, R. D. Nair, and P. A. Ullrich. A conservative semi-Lagrangian multi-tracer transport scheme (CSLAM) on the cubed sphere grid. *J. Comput. Phys.*, 229:1401–1424, 2010.
- [13] A.D. McLaren. Optimal numerical integration on a sphere. *Math. of Comp.*, 17(84):361–383, 1963.
- [14] C. Ronchi, R. Iacono, and P. S. Paolucci. The Cubed Sphere: A new method for the solution of partial differential equations in spherical geometry. *J. Comput. Phys.*, 124:93–114, 1996.
- [15] J. G. Simmonds. *A Brief on Tensor Analysis*. Undergraduate Texts in Math. Springer, 2cd edition, 1994.
- [16] I.H. Sloan and R. S. Womersley. Extremal systems of points and numerical integration on the sphere. *Adv. Comp. Math.*, 21(1-2):107–125, 2004.
- [17] P. A. Ullrich, C. Jablonowski, and B. van Leer. High order finite-volume methods for the shallow-water equations on the sphere. *J. Comput. Phys.*, 229:6104–6134, 2010.

†UNIVERSITÉ DE LORRAINE, DÉPARTEMENT DE MATHÉMATIQUES, F-57045 METZ, FRANCE, ‡C.N.R.S., INSTITUT ELIE CARTAN DE LORRAINE, UMR 7502, F-57045 METZ, FRANCE

*E-mail address:* brice.portelenelle@ensimag.grenoble-inp.fr

*E-mail address:* jean-pierre.croisille@univ-lorraine.fr